

LETTERS

Nanocrystals Used as Masks for Nanolithography

D. Ingert and M. P. Pileni*

*Laboratoire L.M.2.N., U.M.R. CNRS 7070, Université P. et M. Curie (Paris VI),
B.P. 52, 4 Place Jussieu, F-752 31 Paris Cedex 05, France*

Received: March 28, 2003; In Final Form: July 15, 2003

Nowadays, the challenge in nanolithography is the size, the shape, and the cost of the masks. In our laboratory, it has been possible to generate nanocrystals and to assemble them. Indeed, one of the interesting properties of these nanocrystals is their ability to form mesoscopic structures like lines and rings. We have used these two geometries as lithographic masks. Colloidal lithography based on 10 nm ferrite nanocrystals has been done. The nanocrystals are deposited on a silicon wafer covered with resist. Nanocrystals are arranged on the mesoscopic scale. Different patterns such as rings and straight lines made of nanocrystals are obtained. These patterns have been used as masks. The patterned substrate is then etched by reactive ion etching (O_2/SF_6), and the structures (lines and rings) are transferred in the silicon substrate. This indicates that even very small nanocrystals are good candidates as lithographic masks; they can offer different geometries at low cost.

One of the major demands in nanotechnology is the miniaturization of ordering patterns for small devices in microelectronics, communications, and data storage. Besides well-established methods for the fabrication of nanometer-scale structures,¹ such as electron and ion beam lithography, there is a need of alternative simple techniques to save processing time and cost. This need has given rise to different kinds of approaches like, for example, the use of diblock polymers² or self-assembly monolayers (SAMs).^{3,4} Another technique called nanosphere lithography^{5,6} is a useful method for fabricating periodic arrays of submicrometer scale particles. It is the second-generation innovation of the technique originally known as "natural lithography",⁷ where a monodisperse spheres template (typically polystyrene beads with an average diameter of 200 nm) acts as a deposition mask. The present limitations are the production of particles differing by their sizes, shapes, size distributions, and interparticle spacings.

This work is inspired by nanosphere lithography but using nanocrystal organizations as masks.

Due to Bénard-Marangoni instabilities,^{8,9} nanocrystals coated with alkyl chains can self-organize in ringlike structures by using

an antipillary tweezer. Another way to organize magnetic nanocrystals is to apply an external magnetic field during deposition, inducing formation of tubelike structures.^{11–13} In both cases, it is possible to make various patterns on mesoscopic scales.

This paper shows that ferrite nanocrystals can be used as the mask in nanolithography and well-defined mesoscopic structures are, by this method, etched on a substrate.

To pattern substrates with deposited nanocrystals by lithography, three steps must be followed:

- (1) Sample cleaning and resist deposition.
- (2) Controlled deposition of nanocrystals.
- (3) Patterning transfer onto the material by Reactive Ion Etching (RIE).

The samples are cleaned by sonication in detergent, acetone, ethanol, and pure water. About 60 nm of resist, poly(methyl methacrylate) (PMMA), is spin coated on a SiO_2 substrate.

Maghemite nanocrystals coated with lauric acid and with 10 nm average diameter are dispersed in hexane (see appendix I) and deposited on the substrate by using an antipillary tweezer. Before the etching process, the SEM pattern shows that the

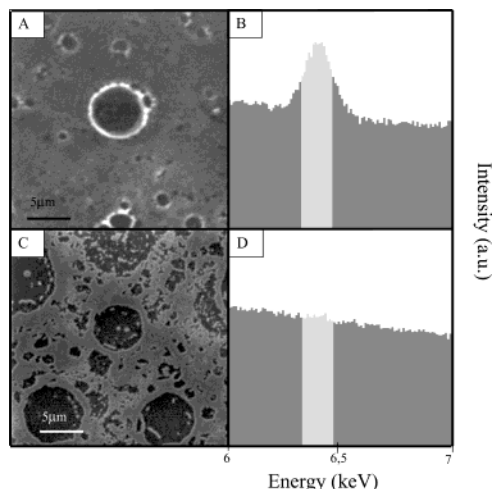


Figure 1. (A) and (B) SEM and EDX patterns of nanocrystals self-organized in rings before etching (process). (C) and (D) SEM and EDX patterns of the sample after etching and washing (process).

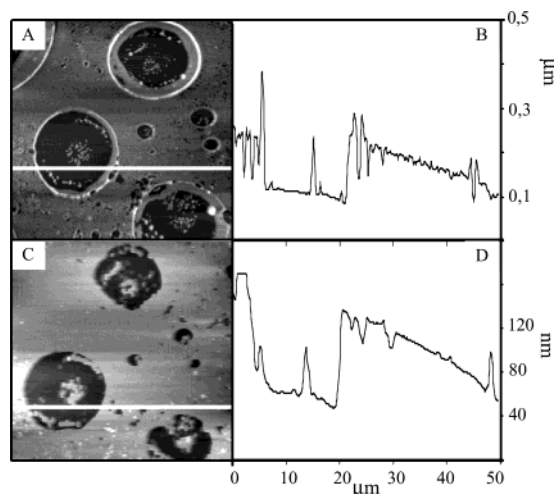


Figure 2. (A) and (B) AFM image and cross section of a ring obtained before etching. (C) and (D) AFM image and cross section of a ring obtained after etching.

nanocrystals self-organize in micrometer rings (Figure 1A). The EDX pattern shows the presence of iron (Figure 1B). The

colored zone corresponds to the main iron peak centered at 6.40 keV ($K\alpha$). The XRD diffractogram characteristic of the maghemite cubic phase is that observed in powder form. The sample is then subjected to an RIE process¹⁴ using O_2 and SF_6 . After etching and washing the sample with ethanol, the SEM pattern (Figure 1C) still shows rings, similar to that observed above (Figure 1A). As can be seen in Figure 1D, no more iron is detected by EDX. The XRD is that of the silicon substrate, the maghemite signal has disappeared. This clearly indicates that the rings observed in Figure 1C are made of Si. This is a direct proof that ferrite nanocrystals are highly efficient for use as a mask. Hence mesostructures can be reproduced in a given substrate through a lithographic mask.

To obtain more precise information on the etching process, AFM patterns are recorded before and after etching. Due to the size distribution of the rings and the fact that AFM is a local measurement, we focus on a given ring before and after etching. The obtained rings are shown in Figure 2A and from the cross section of the given ring, its diameter is 15 μm and its height 200 nm (Figure 2B). After etching and washing the sample, the AFM image (Figure 2C) shows a transferred ring characterized by the same diameter and by a depth close to 80 nm, determined from its cross section (Figure 2D). Hence, the transfer takes place through 140 nm (60 nm of PMMA and 80 nm of SiO_2 wafer). However, a loss in the ring profile resolution is observed compared to that obtained before etching. This is explained by the inhomogeneity in the thickness of the pattern mask. In fact, a sinusoidal thickness profile of the mask induces the increase in the width of the etching replica.¹⁵ From the data presented above, 10-nm maghemite nanocrystals coated with lauric acid are good candidates for use as a mask.

Maghemite nanocrystals coated with citrate ions (see appendix II) are dispersed in aqueous solution. During the deposition process on the Si substrate coated with PMMA (see above), a magnetic field (0.59 T) is applied. The TEM pattern (Figure 3A) shows formation of lines made of nanocrystals. Similar data were obtained previously.^{10–13} The AFM image confirms formation of long tubes (Figure 3B) and, from the cross section, the height of the lines is around 250 nm (Figure 3C). As often observed, the TEM image shows slightly sharper lines than those observed by AFM. After etching and washing the sample, the AFM image clearly shows the same lines (Figure 3D) with 40

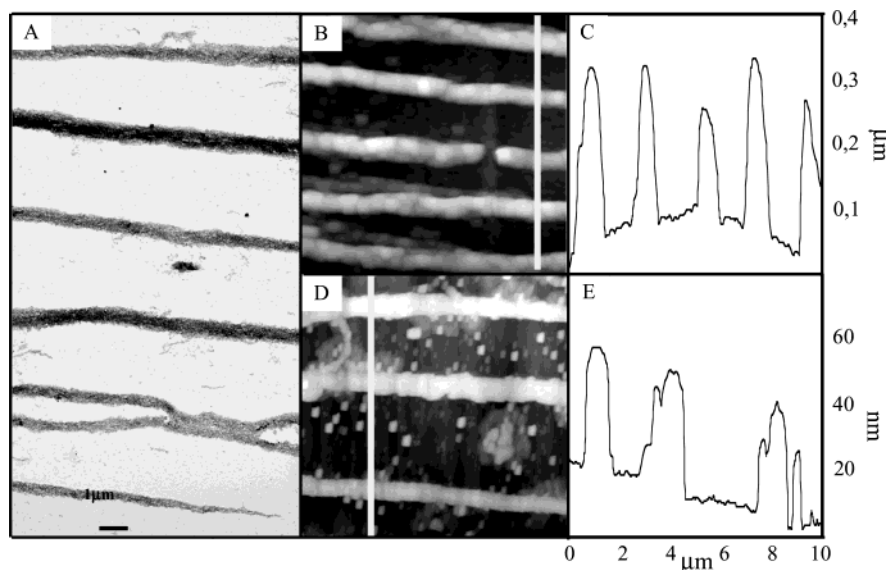


Figure 3. (A) TEM image of lines made of maghemite nanocrystals deposited under a magnetic field. (B) and (C) AFM image and cross section of lines before etching. (D) and (E) AFM image and cross section of lines after etching (process).

nm average depth. As can be seen on the image, the precision of the lines remains almost equivalent before and after etching. This indicates that the resolution transfer improves with increasing the regularity of the mask relief. As with rings, lines made of maghemite nanocrystals play a very efficient role in a transferring mask.

This method permits to demonstrate clearly that 10 nm maghemite nanocrystals are robust enough to be used as a lithographic mask. From our knowledge, this is the first example showing that such low size nanocrystals can be useful for such a purpose. This first approach opens a new way to produce periodic structures. However, most of them are strongly dependent on the substrate used. The only approach we found to demonstrate these nanocrystals could be used as a lithographic mask was to obtain nanocrystal organizations independent of the substrate on which the nanocrystals are deposited. The two organizations valuable in our laboratory were rings and stripes. This explains why these two mesoscopic structures are used. Hence, rings and lines are etched into a silicon substrate. We are aware of the fact that for hundred-nanometer scales, conventional lithography techniques give better results.¹⁶ Our next goal is to organize the nanocrystals in periodic structures and on long term reach the resolution that could never have been obtained by conventional lithography. Indeed, conversely to the present technique, the prospects of other methods for extending lithography do not appear promising.¹⁷

Acknowledgment. We thank Dr. P. A. Albouy for providing XRD diffractograms, Dr. Fermon for giving access to the clean room and lithography equipment, Y. Lalatonne for providing us the maghemite nanocrystals, Dr. Motte for fruitful discussions, and Dr. Ngo for SEM patterns.

Appendix

Dimethylamine, $[(\text{CH}_3)_2\text{NH}_2\text{OH}] = 8.5 \times 10^{-1} \text{ M}$, is added to a micellar solution of ferrous dodecyl sulfate, $[\text{Fe}(\text{DS})_2] = 1.3 \times 10^{-2} \text{ M}$; the mixture is stirred for 2 h. A magnetic

precipitate appears.¹¹ Following this step, two procedures are used depending on the required coating agent.

I. After the precipitate is washed with HNO_3 (10^{-2} M), a sodium citrate ($1.5 \times 10^{-2} \text{ M}$) aqueous solution is added. The solution is sonicated for 2 h. Acetone is used to remove the excess citrate ions. The maghemite nanocrystals coated with citrate ions are dispersed in water.^{12,13}

II. The precipitate is washed with ethanol, and then a solution of lauric acid ($1.4 \times 10^{-1} \text{ M}$) diluted in ethanol is added. The solution is sonicated for 2 h before washing with ethanol. The maghemite nanocrystals coated with lauric acid are dispersed in hexane.^{12,13}

References and Notes

- (1) Martin, J. I.; Nogués, J.; Liu, K.; Vicent, J. L.; Schuller, I. K. *JMMM* **2003**, *256*, 449.
- (2) Spatz, J. P.; Herzog, T.; Mössmer, S.; Zieman, P.; Möller, M. *Adv. Mater.* **1999**, *11*, 149.
- (3) Kim, E.; Xia, Y.; Whitesides, G. M. *Nature* **1995**, *376*, 581.
- (4) Qin, D.; Xia, Y.; Xu, B.; Yang, H.; Zhu, C.; Whitesides, G. M. *Adv. Mater.* **1999**, *11*, 1433.
- (5) Burmeister, F.; Schäfle, C.; Mattes, T.; Böhmisch, M.; Boneberg, J.; Leiderer, P. *Langmuir* **1997**, *13*, 11, 2983.
- (6) Hulteen, J. C.; Van Duyne, R. P. *J. Vac. Sci. Technol. A* **1995**, *13*, 3, 1553.
- (7) Deckmann, H. W.; Dunsmuir, J. H. *Appl. Phys. Lett.* **1982**, *41*, 377.
- (8) Maillard, M.; Motte, L.; Pileni, M. P. *Adv. Mater.* **2001**, *13*, 3, 200.
- (9) Maillard, M.; Motte, L.; Ngo, A. T.; Pileni, M. P. *J. Phys. Chem. B* **2000**, *104*, 11871.
- (10) Ngo, A. T.; Pileni, M. P. *Adv. Mater.* **2000**, *12*, 276.
- (11) Ngo, A. T.; Pileni, M. P. *J. Phys. Chem. B* **2001**, *105*, 1, 53.
- (12) Lalatonne, Y.; Motte, L.; Russier, V.; Ngo, A. T.; Bonville, P.; Pileni, M. P. To be published.
- (13) Lalatonne, Y.; Motte, L.; Pileni, M. P. To be published.
- (14) The reactive ion etching is performed as follows for all the samples: 20 s with O_2 10 cm^3 , $5 \mu\text{bar}$, 30 W and then 30 s with SF_6 10 cm^3 , $5 \mu\text{bar}$, 30 W.
- (15) Huang, C. J.; Zhu, X. P.; Li, C.; Zuo, Y. H.; Cheng, B. W.; Li, D. Z.; Luo, L. P.; Yu, J. Z.; Wang, Q. M. *J. Cryst. Growth* **2002**, *236*, 141.
- (16) Goodberlet, J. G. *Appl. Phys. Lett.* **2000**, *76*, 6, 667.
- (17) Smith, H. I. *Physica E* **2001**, *11*, 104.